

# Neutrino signals from ultracompact minihalos and constraints on the primordial curvature perturbation

Yupeng Yang<sup>1,2,3,\*</sup>, Guilin Yang<sup>1,3,†</sup> and Hongshi Zong<sup>1,3,4‡</sup>

<sup>1</sup>*Department of Physics, Nanjing University, Nanjing, 210093, China*

<sup>2</sup>*Department of Astronomy, Nanjing University, Nanjing, 210093, China*

<sup>3</sup>*Joint Center for Particle, Nuclear Physics and Cosmology, Nanjing, 210093, China*

<sup>4</sup>*State Key Laboratory of Theoretical Physics, Institute of Theoretical Physics, CAS, Beijing, 100190, China*

Compared with that of standard dark matter halos, the density profile of the recently proposed new kind of dark matter structure named ultracompact minihalos (UCMHs) is steeper and its formation time is earlier. If the dark matter is composed of weakly interactive massive particles (WIMP), the potential signals, e.g. neutrinos, from UCMHs due to the dark matter annihilation would be detected by IceCube/DeepCore or other detectors and such signals would have a very useful complementarity of  $\gamma$ -ray observations. On the other hand, the formation of UCMHs is related to primordial curvature perturbations on the smaller scales. So constraints on the abundance of UCMHs can be used to give a limit on the perturbations on these scales. In previous works in the literature, the authors focused on the  $\gamma$ -ray signals from UCMHs due to dark matter annihilation. In this work, we investigate the neutrino signals from nearby UCMHs. Although no excess of neutrino signals the dark matter annihilation has been observed, the constraints on the abundance of UCMHs can be obtained and these constraints can be translated into the limit on the primordial curvature perturbations on small scales.

## I. INTRODUCTION

In the earlier epoch, primordial black holes (PBHs) would be formed if there were large density perturbations ( $\delta\rho/\rho \geq 0.3$ ) [1]. On the other hand, theoretical research and many observations have shown that the present cosmic structures comes from the earlier density perturbations which have smaller amplitude  $\delta\rho/\rho \sim 10^{-5}$  [2]. Recently, Ricotti and Gould proposed that a new kind of structure named ultracompact minihalos (UCMHs) would be formed if the density perturbations satisfy the conditions:  $3 \times 10^{-4} \lesssim \delta\rho/\rho \lesssim 0.3$  [3]. Compared with classical dark matter halos, the formation time of these objects is earlier and the density profile is steeper. So it is expected that these new interesting structures would have an effect on the cosmological evolution, such as reionization and recombination, due to the dark matter annihilation within them if the dark matter is composed of weakly interacting massive particles (WIMP) [4–6], such as neutralinos. According to the theory, dark matter can annihilate into the standard particles, such as photons( $\gamma$ ), electrons and positrons( $e^+$ ,  $e^-$ ), and UCMHs would become one kind of possible high energy astrophysical sources, such as  $\gamma$ -ray sources [7–9]. The other kind of important product of dark matter annihilation is the neutrino. Although this kind of particle has nearly no effect on the process of reionization or recombination, dark matter halos would be the potential neutrino sources [10–12]. According to the present theory and observations,

<sup>1</sup> there are three types of neutrino,  $\nu_e, \nu_\mu, \nu_\tau$ , and they can convert into one another during propagation. The virtue of neutrino detection is that the neutrinos can propagate nearly without attenuation, so the orientation of the sources can be confirmed easily. Among them, muons ( $\mu$ ) can be produced by the charged flux interaction when they propagate through the medium and they can be detected by way of the Cherenkov radiation which is produced when  $\mu$  propagates through a medium such as water. So,  $\nu_\mu$  is the main target particle of the conventional detection. Generally, the production of gamma-ray flux goes with the neutrino signals when the dark matter annihilates. Therefore, the research on neutrino signals would be a good complementarity of gamma-ray detection. In this paper, different from Refs. [7–9] where the authors have focused on the gamma-ray flux, we will investigate the potential neutrino signals from the UCMHs due to dark matter annihilation.

Besides being potential high energy astrophysical sources, UCMHs are related to the primordial power spectrum of density (curvature) perturbations on small scales due to their earlier formation time. On larger scales ( $k \sim 10^{-4} - 1\text{Mpc}^{-1}$ ), the primordial power spectrum of curvature perturbations can be constrained by the CMB, Lyman- $\alpha$  and large scale structure observations [14–17]. All of these observations show a nearly scale-invariant spectrum of primordial perturbations with an amplitude  $\mathcal{P}_{\mathcal{R}}(k) \sim 10^{-9}$ . <sup>2</sup> On smaller scales ( $k \sim 1 - 10^{20}\text{Mpc}^{-1}$ ), the main constraints come from the PBHs,  $\mathcal{P}_{\mathcal{R}}(k) \sim 10^{-2}$  [18]. If the UCMHs are

\* yyp@chenwang.nju.edu.cn

† yanggl@chenwang.nju.edu.cn

‡ zonghs@chenwang.nju.edu.cn

<sup>1</sup> The new constraint on the number of relativistic species coming from the WMAP-9 year data is  $N_{\text{eff}} = 3.26 \pm 0.35$  [13].

<sup>2</sup> The new results from the WMAP-9 year data show that there is a tilt in the primordial spectrum [13].

formed during the earlier epoch, these objects could also be used to obtain the constraints on smaller scales. In Refs. [9, 19], the authors first used the  $\gamma$ -ray observations to obtain the constraints on the abundance of UCMHs for different masses and then obtained the limit on the primordial curvature perturbations for the corresponding scales,  $\mathcal{P}_{\mathcal{R}}(k) \sim 10^{-7} - 10^{-6}$  for  $k \sim 5 - 10^8 \text{Mpc}^{-1}$ . The complementary constraints can also be obtained from the effect of astrometric microlensing produced by UCMHs [20]. In this work, we will use the neutrino observations to obtain the constraints on the primordial power spectrum of curvature perturbations for the small scales.

This paper is organized as follows. The neutrino signals from UCMHs due to dark matter annihilation are studied in Sec. II. In Sec. III, the constraints on the abundance of UCMHs are obtained using the neutrino observations. Then, using these results, we obtain the constraints on the primordial power spectrum of curvature perturbations for the small scales. The conclusions are presented in Sec. IV.

## II. NEUTRINO SIGNALS FROM UCMHs DUE TO THE DARK MATTER ANNIHILATION

### A. The basic quality of UCMHs

After the seeds of UCMHs are formed, the mass will increase through the radial infall. During the radiation dominated epoch, the increase of the mass is slow until after the redshift of equality of radiation and matter. The variation of the mass of UCMHs with the redshift can be written as [7, 21]

$$M_{\text{UCMHs}}(z) = M_i \left( \frac{1 + z_{\text{eq}}}{1 + z} \right), \quad (1)$$

where  $M_i$  is the mass within the perturbations scale at the redshift  $z_{\text{eq}}$ . The density profile of UCMHs can be obtained from the simulation [21, 22],  $\rho \sim r^{-9/4}$ , and the specific form is

$$\rho(r, z) = \frac{3f_{\chi} M_{\text{UCMHs}}(z)}{16\pi R(z)^{\frac{3}{4}} r^{\frac{9}{4}}}, \quad (2)$$

where  $R(z) = 0.019 \left( \frac{1000}{z+1} \right) \left( \frac{M(z)}{M_{\odot}} \right)^{\frac{1}{3}}$  pc and  $f_{\chi} = \frac{\Omega_{DM}}{\Omega_b + \Omega_{DM}} = 0.83$  [2] is the dark matter fraction which describes that only dark matter content collapsed to form the UCMHs in the beginning. Due to the structure formation effect, the mass of UCMHs will stop increasing soon and in this work we assume the corresponding redshift is  $z \sim 10$  [7, 19]. The radius of UCMHs is  $R_{(z=10)} = 0.01 M_i^{\frac{1}{3}}$  and  $R \sim 1$  kpc for  $M_i = 10^6 M_{\odot}$ . So, following the previous works [7, 9, 19], in this paper we also treat the UCMHs as point sources.

### B. Neutrino signals from nearby UCMHs

The annihilation rate of dark matter is proportional to the number density squared,  $\Gamma \sim n^2 \langle \sigma v \rangle = \rho^2 \langle \sigma v \rangle / m^2$ , so the UCMHs have very significant effect on the cosmological evolution [5, 6, 8]. In Refs. [7, 8, 19], the authors have investigated the  $\gamma$ -ray flux from the nearby and extra-Galactic UCMHs. Besides these high energy photons, the neutrinos would be produced together with the  $\gamma$ -ray in the process of dark matter annihilation. There are three flavors of neutrinos and their anti-neutrinos,  $\nu_e(\bar{\nu}_e), \nu_{\tau}(\bar{\nu}_{\tau}), \nu_{\mu}(\bar{\nu}_{\mu})$ , and they can convert into one another due to the vacuum oscillation effect. The muon neutrinos ( $\nu_{\mu}$ ) can convert to muons ( $\mu$ ) during their propagation due to the charged current interaction with the matter. These muon signals can be detected by the detectors on Earth through, for example, the Cherenkov light. Some muons would be produced in the detectors and some are produced before arriving at the detectors. In this paper, we consider these two kinds of neutrino signals which are named contained and upward events, respectively.

The muons produced in the detector through the charged current interactions are called "contained events". Following Ref. [23], this kind of flux can be written as

$$\frac{d\phi_{\mu}}{dE_{\mu}} = \frac{N_A \rho}{2} \int_{E_{\mu}}^m dE_{\nu} \left( \frac{d\phi_{\nu}}{dE_{\nu}} \right) \left( \frac{d\sigma_{\nu}^p(E_{\nu}, E_{\mu})}{dE_{\mu}} + (p \rightarrow n) \right) + (\nu \rightarrow \bar{\nu}) \quad (3)$$

where  $N_A = 6.022 \times 10^{23}$  is Avogadro's number and  $\rho$  is the density of the medium.  $\frac{d\sigma_{\nu, \bar{\nu}}^p}{dE_{\mu}}$  are the scattering cross sections of neutrinos and antineutrinos off protons and neutrons.  $\frac{d\phi_{\nu}}{dE_{\nu}}$  is the differential flux of neutrinos from UCMHs due to the dark matter annihilation

$$\frac{d\phi_{\nu}}{dE_{\nu}} = \frac{1}{8\pi} \frac{dN_{\nu}}{dE_{\nu}} \frac{\langle \sigma v \rangle}{m_{\chi}^2 d^2} \int \rho^2(r) 4\pi r^2 dr, \quad (4)$$

where  $\frac{dN_{\nu}}{dE_{\nu}}$  is the neutrino number per dark matter annihilation and can be obtained from the public code DarkSUSY [24]. In this paper, we consider the ratio between the neutrino flavors as 1:1:1. Here, we have treated UCMHs as point sources and  $d$  is the distance of UCMHs from Earth. The flux of the contained events is shown in the Fig. 1. Two channels ( $\tau^+ \tau^-$ ,  $\mu^+ \mu^-$ ) are shown and the distance is  $d = 10$  kpc. For the mass of UCMHs, we have chosen three values:  $M_{\text{UCMHs}} = 10^{-5}, 1.0$ , and  $10^5 M_{\odot}$ .

The main background of the neutrino signals is the atmospheric neutrino flux. For the spectrum of these flux, we use the form [25, 26]

$$\frac{d\phi_{\nu}}{dE_{\nu} d\Omega} = N_0 E_{\nu}^{-\gamma-1} \times \left( \frac{a}{1 + b E_{\nu} \cos\theta} + \frac{c}{1 + e E_{\nu} \cos\theta} \right), \quad (5)$$

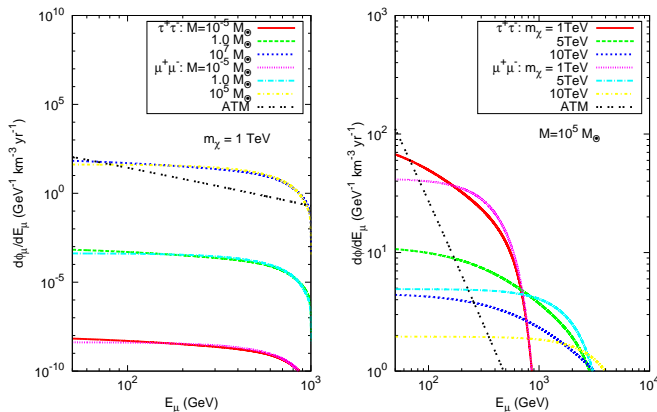


FIG. 1. The contained events of muons from UCMHs due to dark matter annihilation. Two channels are shown:  $\tau^+\tau^-$ ,  $\mu^+\mu^-$ . Left: The dark matter mass is fixed  $m_\chi = 1$  TeV, and the masses of UCMHs are  $M_{\text{UCMHs}} = 10^{-5}, 1.0$  and  $10^5 M_\odot$  respectively. Right: The dark matter masses are  $m_\chi = 1, 5$  and  $10$  TeV and the mass of UCMHs is  $M_{\text{UCMHs}} = 10^5$ . For these results, the cross section of dark matter annihilation has been set as  $\langle\sigma v\rangle = 3.0 \times 10^{-26} \text{cm}^3 \text{s}^{-2}$ . In both figures, the angle-averaged muon's flux ( $\theta_{\text{max}} = 5^\circ$ ) for the atmospheric neutrino is also shown (ATM).

where  $\gamma = 1.74, a = 0.018, b = 0.024, c = 0.0069, e = 0.00139, N_0 = 1.95 \times 10^{17}$  for neutrinos and  $1.35 \times 10^{17}$  for antineutrinos. For the neutrino detector, e.g. the Ice-Cube, the angular resolution is  $\theta = 1^\circ \sim 3^\circ$  for the energy ranges considered by us [27]. On the other hand, the angle between the muon and the neutrino in the neutrino-nucleon scattering should also be considered. Therefore, we set the angle  $\theta_{\text{max}} = 5^\circ$  and it is enough for our work. In addition, it should be noted that the more detailed analysis might lead to an even better signal to background ratio than indicated in this work, especially at higher energies, where smaller opening angles might be possible.

From Fig. 1, one can see that the bigger the masses of UCMHs are, the larger the final muon flux is. For  $M_{\text{UCMHs}} = 10^5 M_\odot$ , the muon flux exceeds the ATM flux which becomes lower for the higher energy. For a fixed mass of UCMHs, the muon flux will be larger for bigger dark matter mass and higher muon energy. Because the flux of ATM decreases as the energy increases, the neutrino signals from UCMHs due to dark matter annihilation would be detected possibly at higher energy for the large dark matter mass.

The muon neutrinos can also convert into muons before arriving at the detector. The flux for this case is called ‘upward events’

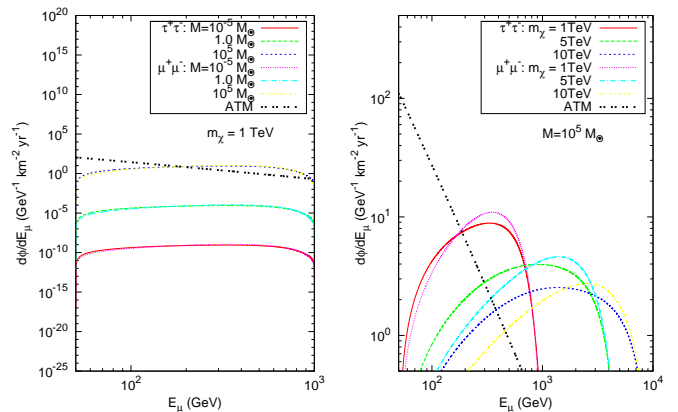


FIG. 2. The upward events of muons from UCMHs due to dark matter annihilation. Here, we have chosen the threshold of the detector to be  $E_\mu^{\text{th}} = 50 \text{GeV}$ . The other related parameters used here are the same as those in Fig. 1.

$$\frac{d\phi_\mu}{dE_\mu} = \frac{N_A \rho}{2} \int dE_\nu \left( \frac{d\phi_\nu}{dE_\nu} \right) \times \left( \frac{d\sigma_\nu^p(E_\nu, E_\mu)}{dE_\mu} + (p \rightarrow n) \right) R(E_\mu) + (\nu \rightarrow \bar{\nu}), \quad (6)$$

where  $R(E_\mu)$  is the distance at which muons can propagate in matter until its energy is below the threshold of the detector  $E_\mu^{\text{th}}$  [12, 28] and its form is  $R(E_\mu) = \frac{1}{\rho\beta} \ln \frac{\alpha + \beta E_\mu}{\alpha + \beta E_\mu^{\text{th}}}$  with  $\rho$  being the density of the medium,  $\alpha \sim 10^{-3} \text{GeVcm}^2/\text{g}$  and  $\beta \sim 10^{-6} \text{cm}^2/\text{g}$ . The upward events from the UCMHs are shown in Fig. 2. From this figure one can see that the muon flux for the fixed dark matter mass (left) is comparable with the contained events. The muons with energy below the threshold of the detector cannot arrive at the detector, so the signals are cut off near the energy  $E \sim 50$  GeV. A common character of the contained and upward events is that the flux of muons from the UCMHs due to the dark matter annihilation exceeds the flux of the atmospheric muons for larger masses of UCMHs and dark matter. For these cases, the UCMHs can possibly be detected.

### C. Comparison with other observations

As we mention in the introduction, previous works focused on the  $\gamma$ -ray signals from the UCMHs. In this section, we will discuss these aspects and it can be seen that although the gamma-ray detection is much more attractive, the neutrino detection is still competitive in some cases. In Ref. [7], the authors studied the  $\gamma$ -ray signals from the nearby UCMHs ( $d_{\text{UCMHs}} = 100 \text{pc}$ ) formed during three phase transitions in the early Universe (electroweak symmetry breaking, QCD confinement and  $e^+e^-$

annihilation). They found that for some cases the integrated flux above 100 MeV exceeds the thresholds of EGRET or Fermi. For example, for the  $b\bar{b}$  channel, the  $\gamma$ -ray signals from the UCMHs formed during the  $e^+e^-$  annihilation period exceed the threshold of EGRET and Fermi for the dark matter mass  $m_\chi \sim 10 - 1000\text{GeV}$ . For the lepton channel,  $\mu^+\mu^-$ , the flux is lower but still above the threshold value. So, if there are UCMHs within this distance, they would be observed by Fermi. In order to have a comparison with our results, we find that the integrated gamma-ray flux for the  $\mu^+\mu^-$  channel in Ref. [7] will be rescaled by a factor  $\sim 10^{-2}$  for  $d \sim 10\text{kpc}$  and  $M_{\text{UCMHs},0} \sim 10^5 M_\odot$ . As a result, the flux will be under the threshold of the EGRET or Fermi detectors for the larger dark matter mass, e.g.  $m_\chi \sim 1\text{TeV}$ . The situations are different for the neutrino signals. As shown in the left plot in Fig. 1, the neutrino signals from the UCMHs are still larger than the ATM. From the right plot it can also be seen that the situation is much better for the larger dark matter mass. But it should be noticed that for the lighter dark matter e.g.  $m_\chi \sim 100\text{GeV}$ , due to the stronger flux of ATM, the gamma-ray detection are much more competitive than the neutrino case. Other interesting targets which are similar to the UCMHs are the dwarf spheroidals which are confirmed to be dark matter dominated. In Ref. [29], the potential  $\gamma$ -ray flux is studied using the Fermi-LAT detector. No obvious excess has been observed and these nondetection results can be transformed into the limits on the dark matter parameters, e.g. dark matter mass ( $m_\chi$ ) and the thermal averaged annihilation cross section ( $\langle\sigma v\rangle$ ). The limits are different for different dark matter models and different dwarf spheroidals. The neutrino signals have also been studied using the IceCube detector and there is no excess of signals [30]. The limits on the dark matter parameters can also be derived from these results. It can be seen that for the neutrino signals the constraints are weaker. On the other hand, the  $\gamma$ -ray and the neutrino signals are channel dependent. The constraints on the dark matter from the  $\gamma$ -ray detection are stronger for  $b\bar{b}$  or  $W^+W^-$  channels. One main reason for this is that the integrated number of these channels is larger than that of the lepton channels. The situation is different for the neutrino detection and the limits are stronger for the  $\mu^+\mu^-$  and  $\tau^+\tau^-$  channels. For example, the authors of [28] studied the neutrino signals from nearby dwarfs. They found that compared with the current gamma-ray detectors, for the  $\mu^+\mu^-$  or  $\nu_\mu\bar{\nu}_\mu$  channels, the IceCube neutrino detector will be competitive, especially for large dark matter mass,  $m_\chi \gtrsim 7\text{TeV}$ . Similar results can also be seen from Refs. [30, 31]. For the neutrino detection, the main contamination for the source signals is from the atmospheric neutrino flux. From Eq. 5 it can be seen that these flux decreases with increasing energy as  $\sim E_\nu^{-3}$ . On the other hand, the muon flux from the UCMHs does not decrease as much. So the neutrino signals would be detected for higher energy which corresponds to the larger dark matter mass or UCMHs. On top of this, with the improve-

ment of the angular resolution of neutrino telescopes, it is expected that the limits on dark matter will be much better. Therefore, compared with the gamma-ray detectors, the neutrino detection has its own advantage, especially for heavier dark matter (e.g.  $m_\chi \gtrsim 1\text{TeV}$ ) and lepton channels (e.g.  $\mu^+\mu^-$  or  $\nu_\mu\bar{\nu}_\mu$ ). The other most important point is that they will be a very useful complementarity of  $\gamma$ -ray observations for seeking dark matter.

### III. CONSTRAINTS ON THE PRIMORDIAL CURVATURE PERTURBATION

The primordial curvature perturbation is very important for modern cosmology and its amplitude can be limited from different observations. The main constraints come from the cosmic microwave background (CMB)  $\mathcal{P}_{\mathcal{R}}(k) \sim 10^{-9}$  [14]. These constraints carry the information of primordial curvature perturbations which correspond to the scales  $k \sim 10^{-4} - 1\text{Mpc}^{-1}$ . For smaller scales, the main constraints come from the PBHs in spite of no observations of these objects,  $\mathcal{P}_{\mathcal{R}}(k) \sim 10^{-2}$  for  $k \sim 10^{-2} - 10^{19}\text{Mpc}^{-1}$  [18]. The UCMHs provide another way of constraining the primordial curvature perturbations on smaller scales. Due to the steep density profile of UCMHs, it is expected that the  $\gamma$ -ray flux would be produced from dark matter annihilation. In order to be consistent with the present observations, such as *Fermi*, the abundance of UCMHs must be constrained. In Refs. [9, 19], the authors used the points sensitivity of *Fermi* to obtain the final constraints,  $\mathcal{P}_{\mathcal{R}}(k) \sim 10^{-6} - 10^{-8}$  for  $k \sim 5 - 10^{7.5}\text{Mpc}^{-1}$ . As mentioned in the introduction, the neutrinos are usually produced together with the  $\gamma$ -ray flux. Therefore, these signals would be a significant complementarity of  $\gamma$ -ray detection. Different from the previous works, we study the potential neutrino signals from UCMHs due to dark matter annihilation. Because no excess of neutrino signals has been observed as compared with the ATM, we can obtain the conservative constraints on the abundance of UCMHs and they can be used to obtain the limit on the primordial curvature perturbations. The methods used by us are mainly from Refs. [9, 19, 20] and here we only show the main description of the calculations.

The cosmological mass fraction at horizon entry,  $\beta(M_H)$ , which then forms the UCMHs, is related to the present fraction of UCMHs [19, 20],

$$\Omega_{\text{UCMHs}} = \Omega_{\text{DM}} \frac{M_{\text{UCMHs}}(z=0)}{M_{\text{UCMHs}}(z_{\text{eq}})} \beta(M_H), \quad (7)$$

where  $\Omega_{\text{UCMHs}}$  and  $\Omega_{\text{DM}}$  are the fractions of UCMHs and DM, respectively,  $M_{\text{UCMHs}}(z=0, z_{\text{eq}})$  is the mass of UCMHs at present and the redshift of equality of matter and radiation. If the initial perturbations are Gaussian, the present fraction of UCMHs can be written in the form [9]

$$\Omega_{\text{UCMHs}} = \frac{2\Omega_{\text{DM}}}{\sqrt{2\pi}\sigma_H(R)} \frac{M(z=0)}{M(z_{\text{eq}})} \times \int_{\delta_{\text{min}}}^{\delta_{\text{max}}} \exp\left(-\frac{\delta_H^2(R)}{2\sigma_H^2(R)}\right) d\delta_H(R), \quad (8)$$

where  $\delta_{\text{max}}$  and  $\delta_{\text{min}}$  are the maximal and minimal values of density perturbations required for the formation of UCMHs. Both of them depend on the redshift [19] and in this work, for simplicity, we choose these values as  $\delta_{\text{max}} = 0.3$  and  $\delta_{\text{min}} = 10^{-3}$ , respectively.  $\sigma_H(R)$  is related to the curvature perturbation as [19, 20]

$$\sigma_H^2(R) = \frac{1}{9} \int_0^\infty x^3 W^2(x) \mathcal{P}_{\mathcal{R}}(x/R) T^2(x/\sqrt{3}) dx, \quad (9)$$

where  $W(x) = 3x^{-3}(\sin x - x\cos x)$  is the Fourier transform of the top-hat windows function with  $x \equiv kR$ .  $T$  is the transfer function describing the evolution of perturbations. For more detailed discussions one can see the appendixes in Refs. [19, 20]. The fraction of UCMHs can be defined as [9]

$$\frac{\Omega_{\text{UCMHs}}}{\Omega_{\text{DM}}} = \frac{M_{\text{UCMHs}}(z=0)}{M_{\text{DM}}(r < d_{\text{obs}})}, \quad (10)$$

where  $M_{\text{DM}}(r < d_{\text{obs}})$  is the mass within the radius  $d_{\text{obs}}$  which is the distance on which the neutrino signals from UCMHs would be observed by the detector. In this work, we use the NFW profile for the dark matter halo of the Milky Way and assume that the abundance of UCMHs is the same everywhere.<sup>3</sup> Much more accurate definition is given in Refs. [32, 33].

The detection of neutrino signals is more difficult than that of the gamma rays due to the weak interactions between neutrinos and other particles. Moreover, the ATM would contaminate the target signals. In order to reduce this effect, Earth itself is usually used as the shield, which means that the good targets should lie on the other side of Earth compared to the detectors. Therefore, for the fixed target one should consider which detector is good. In this work, we assume that the UCMHs studied by us just lie in the appropriate direction. At present or in the near future, there are several detectors which can be used to search neutrino signals, such as IceCube/DeepCore and KM3Net.<sup>4</sup>

Considering the contamination of ATM, for an exposure time such as ten years, the minimal number of neutrinos from UCMHs which satisfies, e.g.  $2\sigma$  statistic significance, can be obtained through [34]

$$T_{\text{obs}} = \sigma^2 \frac{N_{\text{ATM}} + N_{\text{UCMHs}}}{N_{\text{UCMHs}}^2}, \quad (11)$$

where  $N_{\text{UCMHs}}$  is the number of neutrinos from UCMHs due to dark matter annihilation. It can be obtained by integration of Eqs.(3) and (6)

$$N_{\text{UCMHs}} = \int_{E_\mu^{\text{th}}}^{E_{\text{max}}} \frac{d\phi_\mu}{dE_\mu} F_{\text{eff}}(E_\mu) dE_\mu, \quad (12)$$

where  $F_{\text{eff}}(E_\mu)$  correspond to the effective volume  $V_{\text{eff}}$  and effective area  $A_{\text{eff}}$  of the detector for the contained and upward events, respectively. For IceCube/DeepCore, we accept that the energy independent effect volume is  $V_{\text{eff}} = 0.04\text{km}^3$  and the angle-averaged muon effective area is  $A_{\text{eff}} = 1\text{km}^2$ . From Figs. 1 and 2, it can be seen that the neutrino fluxes for the two channels  $\tau^+\tau^-$  and  $\mu^+\mu^-$  are slightly different, but the final integrated number is nearly the same. So, in this work, for simplicity we only consider one channel. The final constraints on the primordial curvature perturbation are shown in Fig. 3. For this plot, we have chosen two values of the dark matter mass,  $m_\chi = 1$  and  $10$  TeV, and the exposure time of the detector is ten years. From this figure, one can see that on the larger scales,  $k \lesssim 10^3\text{Mpc}^{-1}$ , the constraints are nearly the same for different events and dark matter mass. The results are obviously different on larger scales  $10^3 \lesssim k \lesssim 10^8\text{Mpc}^{-1}$ . Stronger constraints come from the upward events and larger dark matter mass. For the contained events, the strongest constraint is  $\mathcal{P}_{\mathcal{R}}(k) \sim 10^{-7.5}$  for  $k \sim 10^3\text{Mpc}^{-1}$ , while for the upward events, the strongest constraint is  $\mathcal{P}_{\mathcal{R}}(k) \sim 10^{-7.6}$  for  $k \sim 10^{3.5}\text{Mpc}^{-1}$ .

#### IV. CONCLUSION

Due to the steep density profile of UCMHs, it is expected that the dark matter annihilation rate is very strong within these objects. The  $\gamma$ -ray flux as the product of dark matter annihilation has been discussed by several authors. On the other hand, neutrinos would be produced together with the gamma rays. In this work, we have studied this kind of potential signal including upward events and contained events. We found that for the fixed distance of UCMHs ( $d = 10$  kpc) the final muon flux would exceed the flux for the ATM case for the large mass of UCMHs (e.g.  $M_{\text{UCMHs}} \sim 10^5 M_\odot$ ) and dark matter (e.g.  $m_\chi \sim 10^4\text{GeV}$ ). Because the flux of ATM decreases as the energy increases, the detection of high energy neutrinos is very significant for the indirect search of dark matter. On the other hand, compared with the classical dark matter halos, the formation time of UCMHs is earlier, so the abundance of UCMHs can be used to constrain the primordial curvature perturbations on small scales, which are not achieved through CMB

<sup>3</sup> For different density profiles of dark matter halos, the final constraints would be different [35]. On the other hand, similar to the PBH case [36, 37], UCMH clusters would be formed during the earlier epoch.

<sup>4</sup> [http://en.wikipedia.org/wiki/List\\_of\\_neutrino\\_experiments](http://en.wikipedia.org/wiki/List_of_neutrino_experiments).

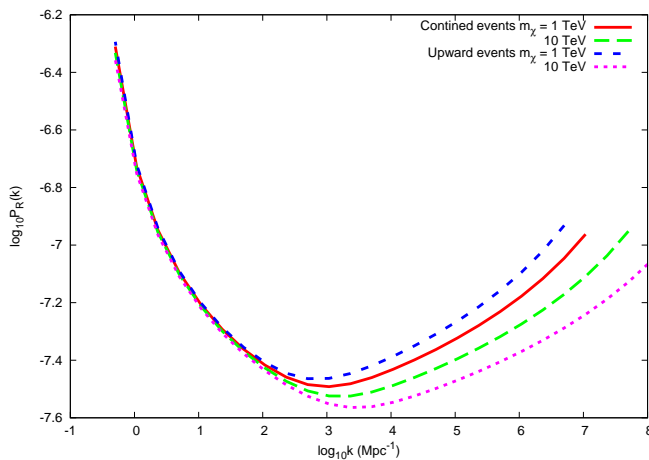


FIG. 3. The constraints on the primordial curvature perturbations on the scales  $k \sim 1 - 10^8 \text{Mpc}^{-1}$ . Here we have set 10 years exposure time for IceCube/DeepCore and  $2\sigma$  statistical significance for ATM. Constraints for both upward and contained events are shown. Two kinds of dark matter mass are considered:  $m_\chi = 1 \text{ TeV}$  and  $10 \text{ TeV}$ .

observations. In the previous works in the literature, the authors obtained the constraints using the  $\gamma$ -ray observations or through the microlensing effect. The neutrino signals as a useful complementarity of gamma rays can also be used to achieve this goal. In this work, comparing with the neutrino background from the atmosphere, we obtain the constraints on the neutrino numbers from

UCMHs due to dark matter annihilation and use these results to obtain the limit on the primordial curvature perturbations on the scales  $k \sim 1 - 10^9 \text{Mpc}^{-1}$ . For the contained events, the strongest limit is  $\mathcal{P}_R(k) \sim 10^{-7.5}$  for  $k \sim 10^3 \text{Mpc}^{-1}$ , and for the upward events, the strongest limit is  $\mathcal{P}_R(k) \sim 10^{-7.6}$  for  $k \sim 10^{3.5} \text{Mpc}^{-1}$ . In the previous works [9, 19], the limits on the primordial curvature perturbations for the smaller scales are also obtained for the nondetection of gamma-ray signals. The strongest limits are  $\mathcal{P}_R(k) \sim 10^{-7}$  and our results are slightly stronger than these limits. However, it should be noted that different formation times of UCMHs also affect the final results (Fig.5 in Ref.[19]). For future detectors, such as KM3Net, due to their larger effective volume (or area) and lower threshold, it is expected that the constraints on the primordial curvature perturbations on small scales will be stronger.

## V. ACKNOWLEDGMENTS

We thank Weimin Sun for improving the manuscript. Yupeng Yang thanks Xiangyu Wang, Lei Feng and Qiang Yuan for useful discussion. This work is supported in part by the National Natural Science Foundation of China (under Grants No. 10935001, 11275097 and No. 11075075) and the Research Fund for the Doctoral Program of Higher Education (under Grant No 2012009111002)

- 
- [1] A. M. Green, A. R. Liddle, *Phys. Rev. D* **56**, 6166 (1997)
  - [2] E. Komatsu et al, *Astron. J. Suppl.* **192**, 18 (2011)
  - [3] M. Ricotti, A. Gould, *Astrophys. J.* **707**, 979 (2009), arXiv:0908.0735
  - [4] D. Zhang, *MNRAS* **418**, 1850 (2011), arXiv:1011.1935
  - [5] Y. Yang, X. Huang, X. Chen, H. Zong, *Phys. Rev. D* **84**, 043506 (2011)
  - [6] Y. Yang, X. Chen, T. Lu, H. Zong, *Eur. Phys. J. Plus* **126**, 123 (2011)
  - [7] P. Scott, S. Sivertsson, *Phys. Rev. Lett.* **103**, 211301 (2009)
  - [8] Y. Yang, L. Feng, X. Huang, X. Chen, T. Lu, H. Zong, *JCAP* **12**, 020 (2011)
  - [9] A. S. Josan, A. M. Green, *Phys. Rev. D* **82**, 083527 (2010), arXiv:1006.4970
  - [10] J. Hisano, K. Nakayama, M. J. S. Yang, *Phys. Lett. B* **678**, 101 (2009), arXiv:0905.2075
  - [11] A. E. Erkoca, M. H. Reno, I. Sarcevic, *Phys. Rev. D* **80**, 043514 (2009), arXiv: 0906.4364
  - [12] Q. Yuan, P. Yin, X. Bi, X. Zhang, S. Zhu, *Phys. Rev. D* **82**, 023506 (2010), arXiv:1002.0197
  - [13] G. Hinshaw et al, arXiv:1212.5226
  - [14] D. Larson et al, *Astron. J. Suppl.* **192**, 16 (2011), arXiv:1001.4635
  - [15] R. Hlozek et al, arXiv:1105.4887
  - [16] S. Bird, H. V. Peiris, M. Viel, L. Verde, *MNRAS* **413**, 1717 (2011), arXiv:1010.1519
  - [17] J. L. Tinker et al, *Astrophys. J.* **745**, 16 (2012)
  - [18] A. S. Josan, A. M. Green, K. A. Malik, *Phys. Rev. D* **79**, 103520 (2009), arXiv:0903.3184
  - [19] T. Bringmann, P. Scott, Y. Akrami, *Phys. Rev. D* **85**, 125027 (2012), arXiv:1110.2484
  - [20] F. Li, A. L. Erickcek, N. M. Law, *Phys. Rev. D* **86**, 043519 (2012), arXiv:1202.1284
  - [21] J. A. Fillmore, P. Goldreich, *Astrophys. J.* **281**, 1 (1984)
  - [22] E. Bertschinger, *Astron. J. Suppl.* **58**, 39 (1985)
  - [23] A. E. Erkoca, M. H. Reno, I. Sarcevic, *Phys. Rev. D* **80**, 043514 (2009), arXiv:1009.2068
  - [24] <http://www.physto.se/~edsjo/darksusy/>
  - [25] T.K. Gaisser, M. Honda, *Ann. Rev. Nucl. Part. Sci.* **52**, 153 (2002)
  - [26] M. Honda, T. Kajita, K. Kasahara, S. Midorikawa, T. Sanuki, *Phys. Rev. D* **75**, 043006 (2007)
  - [27] J. Dumm, H Landsman for the IceCube Collaboration, *J. Phys.: Conf. Ser.* **60**, 334 (2007)
  - [28] P. Sandick, D. Spolyar, M. Buckley, K. Freese, D. Hooper, *Phys. Rev. D* **81**, 083506 (2010), arXiv:0912.0513
  - [29] The Fermi-LAT Collaboration, *Astrophys. J.* **712**, 147 (2010)
  - [30] The IceCube Collaboration, arXiv:1111.2738

- [31] The Fermi-LAT Collaboration, *Phys. Rev. Lett.* **107**, 241302 (2011), arXiv:1108.3546
- [32] T. Bringmann, P. Scott and Y. Akrami, *Phys. Rev. D* **85**, 125027 (2012)
- [33] S. Shandera, A. L. Erickcek, P. Scott and J. Y. Galarza, arXiv:1211.7361
- [34] L. Bergstrom, J. Edsjo, M. Kamionkowski, *Astropart. Phys.* **7**, 147 (1997)
- [35] Y. Yang, Guilin Yang, Hongshi Zong, arXiv:1210.1409
- [36] J. R. Chisholm, *Phys. Rev. D* **73**, 083504 (2006), astro-ph/0509141
- [37] J. R. Chisholm, *Phys. Rev. D* **84**, 124031 (2011), arXiv:1110.4402